

**Supporting Information:**

**Sulfated Alginate as an Effective Polymer Binder for High-Voltage  $\text{LiNi}_{0.5}\text{Mn}_{1.5}\text{O}_4$   
Electrodes in Lithium-Ion Batteries**

Asako Oishi,<sup>†</sup> Ryoichi Tatara,<sup>†</sup> Eiichi Togo,<sup>‡</sup> Hiroshi Inoue,<sup>‡</sup> Satoshi Yasuno,<sup>¶</sup> Shinichi Komaba<sup>†\*</sup>

<sup>†</sup>*Department of Applied Chemistry, Tokyo University of Science, 1-3 Kagurazaka, Shinjuku, Tokyo 162-8601, Japan*

<sup>‡</sup>*Tosoh Corp., 1-8 Kasumi, Yokkaichi-Shi, Mie 510-8540, Japan*

<sup>¶</sup>*Japan Synchrotron Radiation Research Institute, 1-1-1 Kouto, Sayo-gun, Hyogo, 679-5198, Japan*

*\*Email: komaba@rs.tus.ac.jp*

Calculation to obtain sulfation efficiency in Table 1:

Unit mass of ALG: 176.06 [g/mol]

Unit mass of ALG-SO<sub>3</sub> with x% sulfation efficiency: 176.06+160.13x [g/mol]

As we have relationship as follows:

$(64.13x/(176.06+160.13x)) \times 100 = \text{sulfur content [wt\%, elemental analysis]}$

Through solving above equation for x, we obtain sulfation efficiency.

Unit mass of ester-ALG: 234.09 [g/mol]

Unit mass of ester-ALG-SO<sub>3</sub> with x% sulfation efficiency: 234.09+240.195x [g/mol]

As we have relationship as follows:

$(234.09x/(234.09+240.195x)) \times 100 = \text{sulfur content [wt\%, elemental analysis]}$

Through solving above equation for x, we obtain sulfation efficiency.

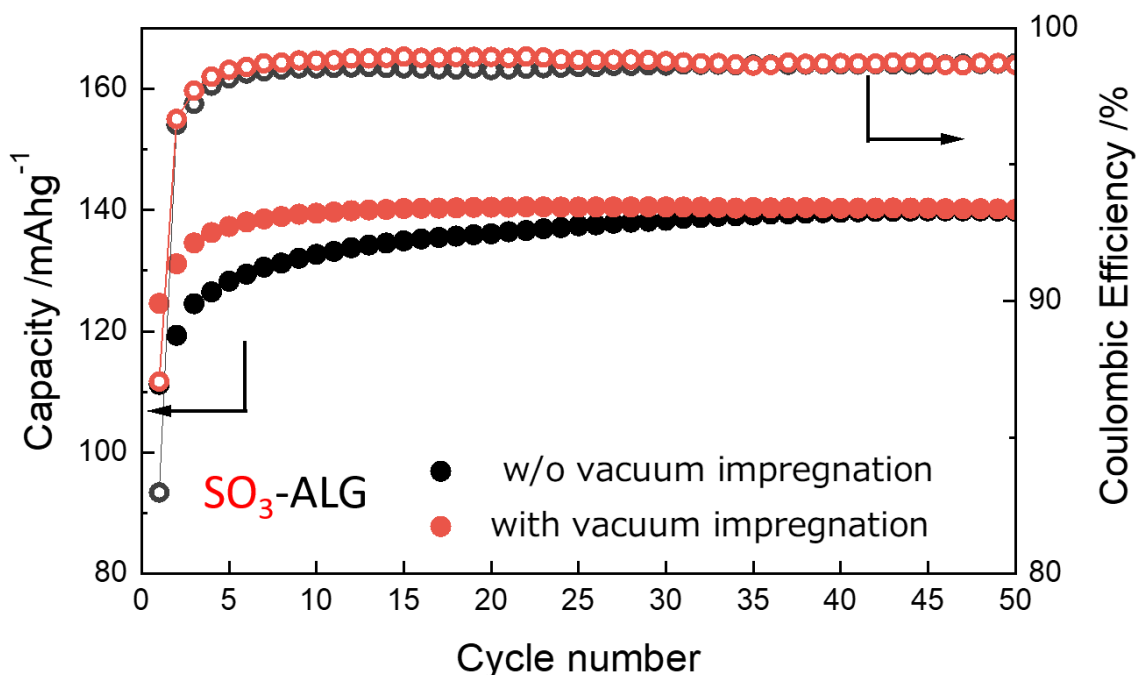


**Figure S1.** Variation of the capacities and Coulombic efficiencies of LNMO//Li half cells with SO<sub>3</sub>-ALG binders, with and without electrolyte vacuum impregnation process. The cells were cycled in the voltage range of 3.5–5.0 V at 20 mA g<sup>-1</sup> at 25 °C using 1 M LiPF<sub>6</sub> in EC/DMC as an electrolyte.

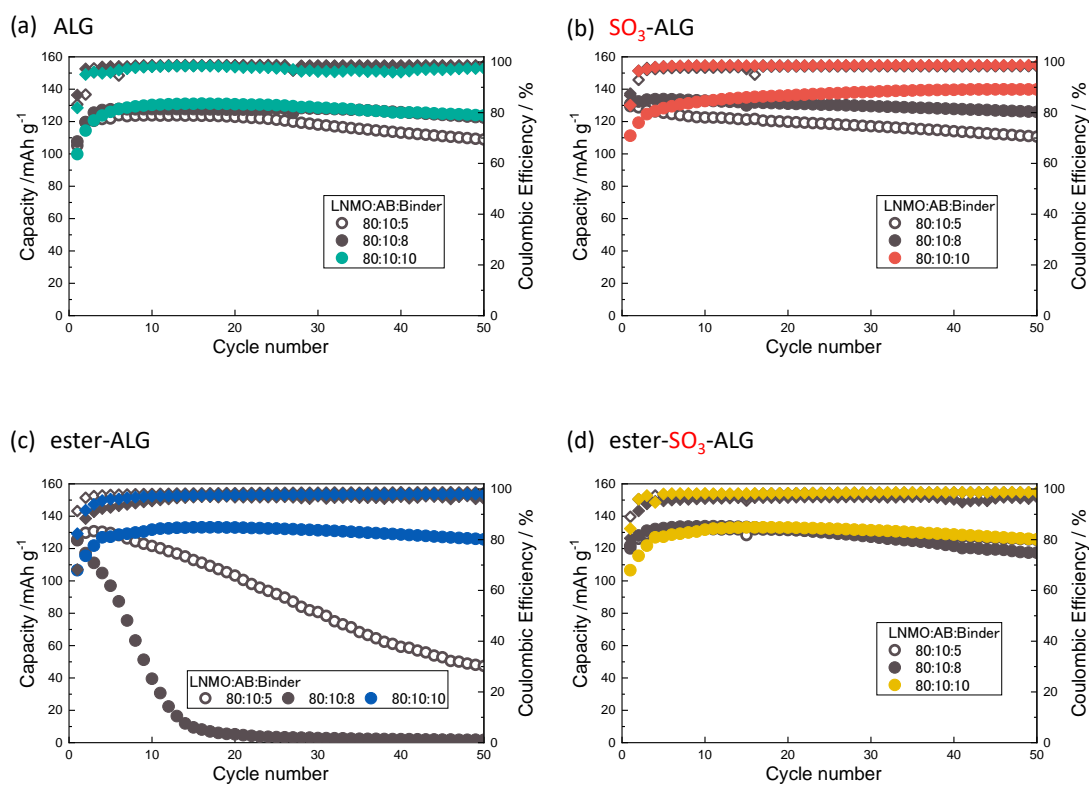


**Figure S2.** Variation of the capacities and Coulombic efficiencies of LNMO//Li half cells with (a) ALG, (b) SO<sub>3</sub>-ALG, (c) ester-ALG, and (d) ester-SO<sub>3</sub>-ALG binders, at different binder polymer contents in the composite electrodes. The cells were cycled in the voltage range of 3.5–5.0 V at 20 mA g<sup>-1</sup> at 25 °C using 1 M LiPF<sub>6</sub> in EC/DMC as an electrolyte.

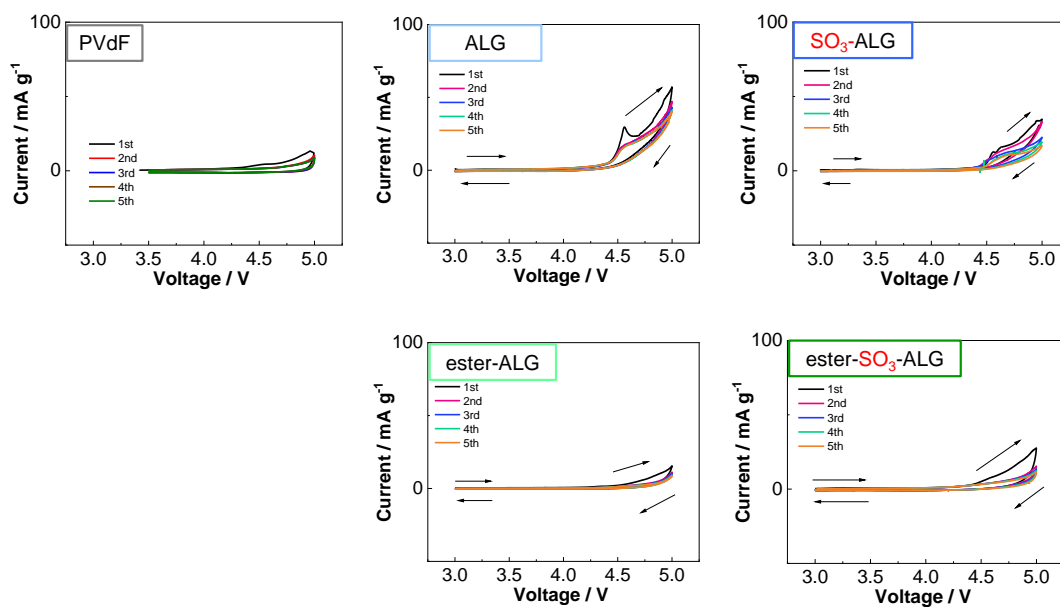


**Figure S3.** Cyclic voltammograms of the LNMO-free composite electrode containing 80% AB and 20% binders cycled in the voltage range of 3.0–5.0 V at  $0.25 \text{ mV s}^{-1}$  at  $25 \text{ }^\circ\text{C}$  using 1 M  $\text{LiPF}_6$  in EC/DMC as an electrolyte.

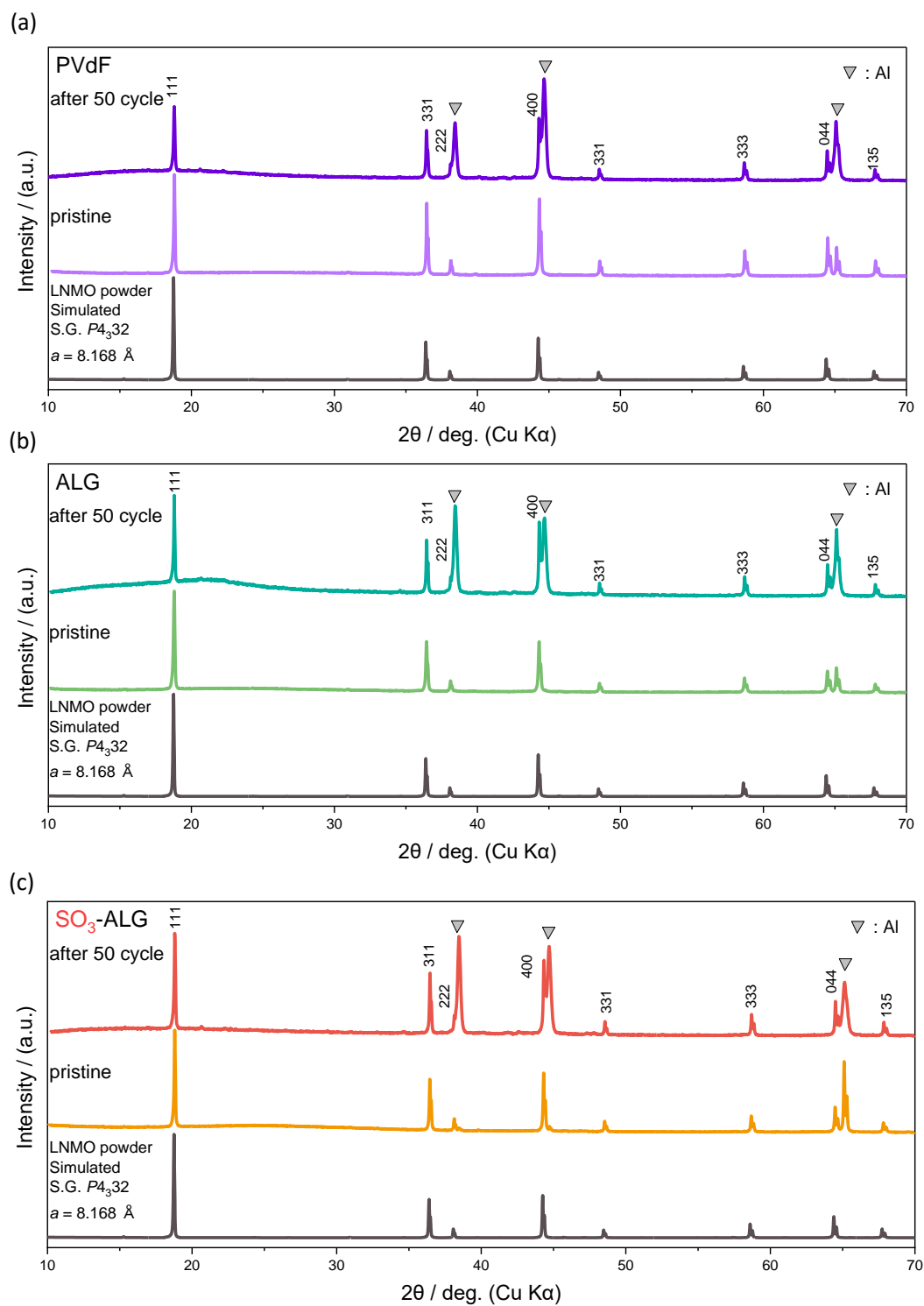


**Figure S4.** XRD patterns of  $\text{LiNi}_{0.5}\text{Mn}_{1.5}\text{O}_4$  electrodes with (a) PVdF, (b) ALG, and (c)  $\text{SO}_3$ -ALG binders recorded before and after cycling.

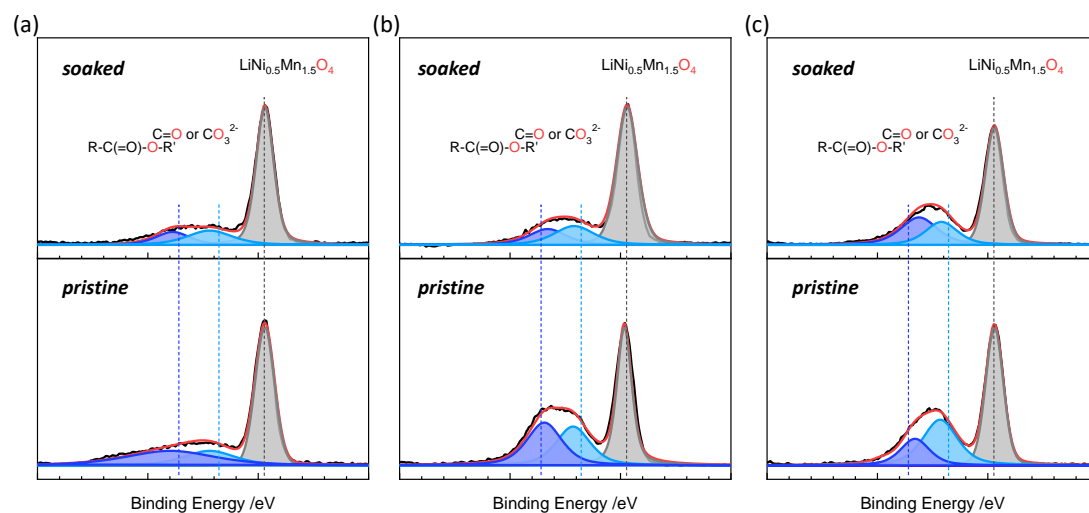


**Figure S5.** O 1s HAXPES profiles of pristine and electrolyte (1 M  $\text{LiPF}_6$  in EC/DMC)-soaked  $\text{LiNi}_{0.5}\text{Mn}_{1.5}\text{O}_4$  electrodes with (a) PVdF, (b) ALG, and (c)  $\text{SO}_3$ -ALG binders.

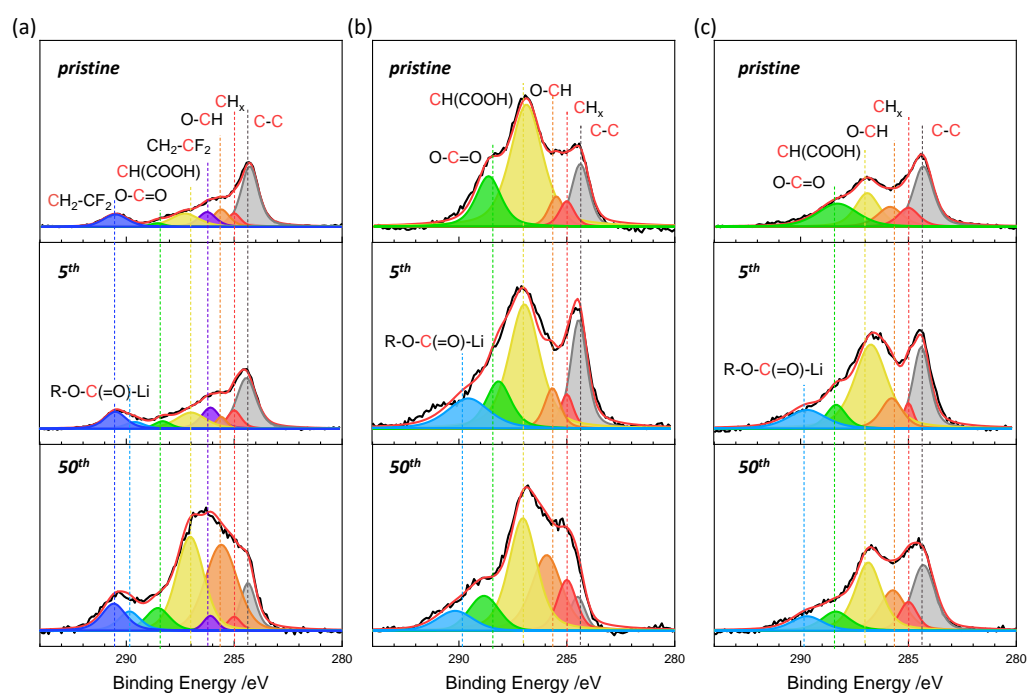


**Figure S6.** C 1s SOXPES profiles of  $\text{LiNi}_{0.5}\text{Mn}_{1.5}\text{O}_4$  electrodes with (a) PVdF, (b) ALG, and (c)  $\text{SO}_3$ -ALG binders recorded before and after cycling.

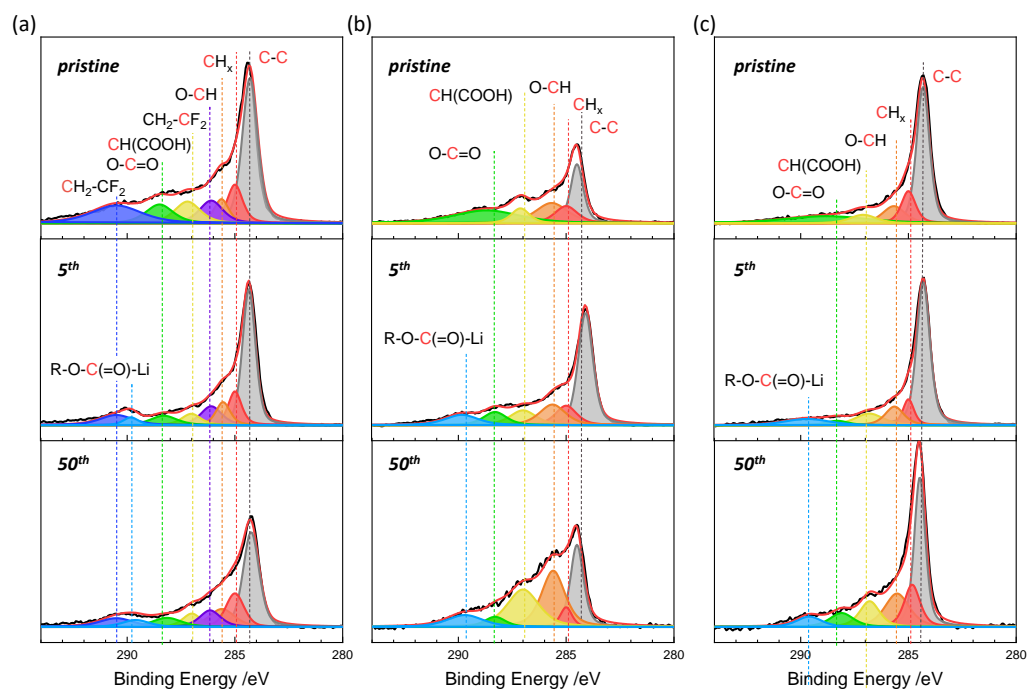


**Figure S7.** C 1s HAXPES profiles of  $\text{LiNi}_{0.5}\text{Mn}_{1.5}\text{O}_4$  electrodes with (a) PVdF, (b) ALG, and (c)  $\text{SO}_3$ -ALG binders recorded before and after cycling.

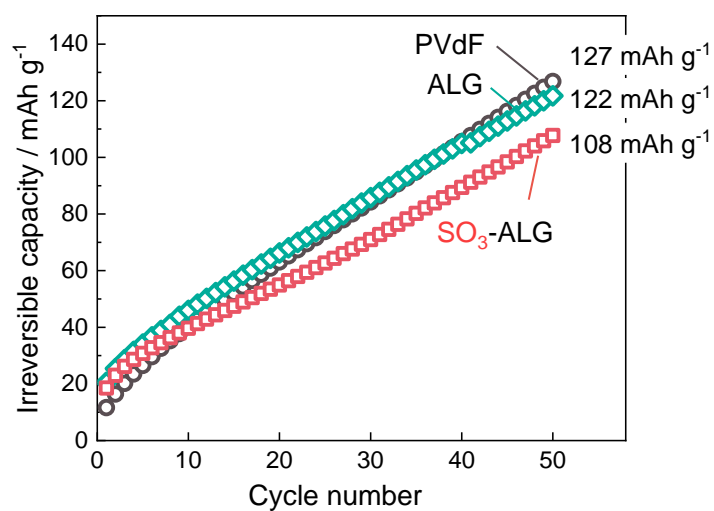


**Figure S8.** Effects of cycling on the irreversible capacity of  $\text{LiNi}_{0.5}\text{Mn}_{1.5}\text{O}_4//\text{Li}$  half cells with PVdF, ALG, and  $\text{SO}_3$ -ALG binders.

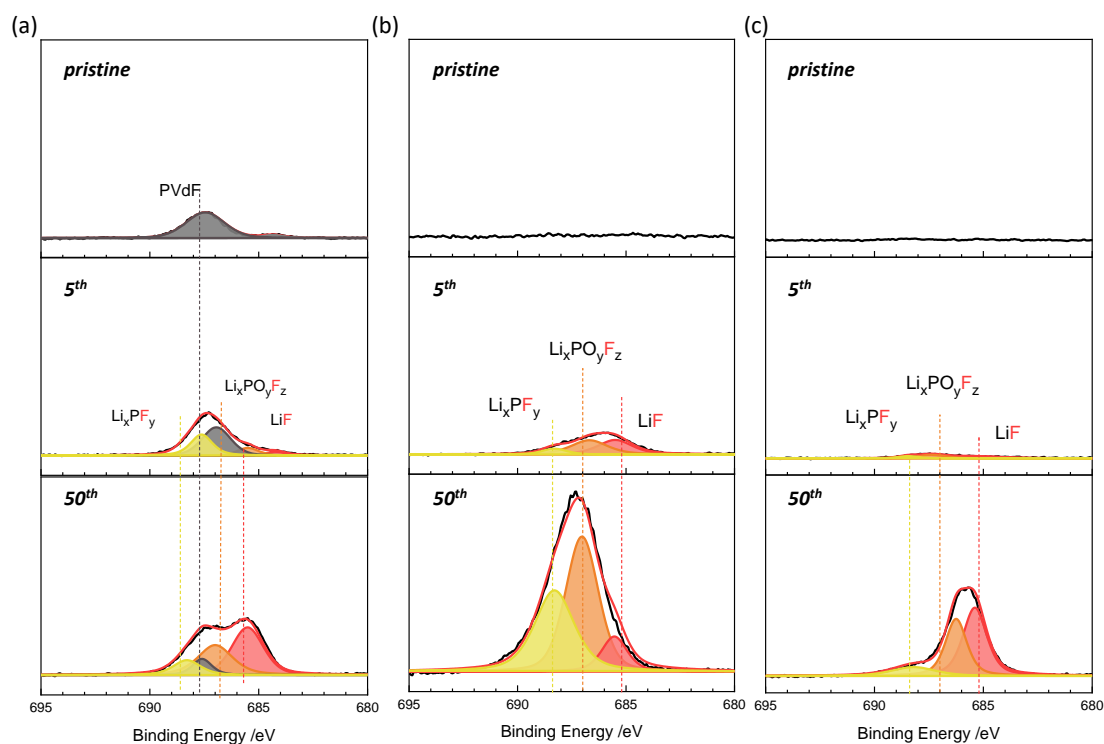


**Figure S9.** F 1s HAXPES profiles of  $\text{LiNi}_{0.5}\text{Mn}_{1.5}\text{O}_4$  electrodes with (a) PVdF, (b) ALG, and (c)  $\text{SO}_3$ -ALG binders recorded before and after cycling.

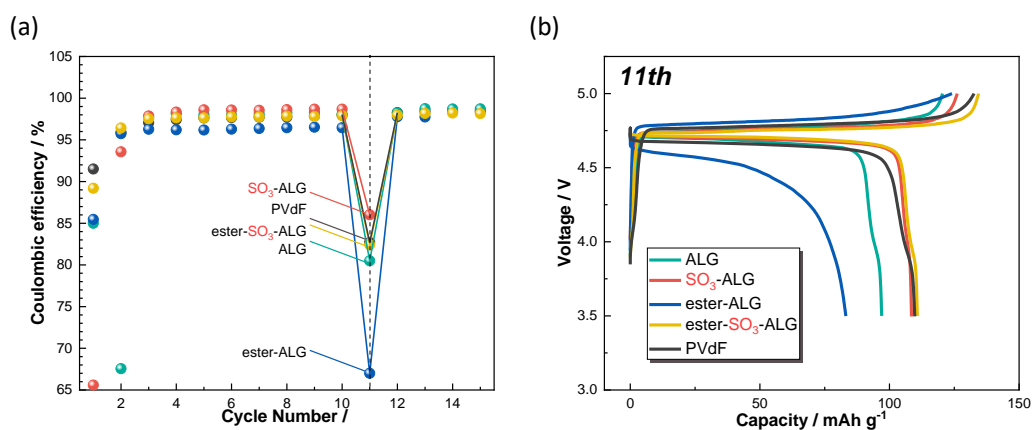


**Figure S10.** (a) Coulombic efficiencies and (b) eleventh-cycle charge–discharge curves obtained during the self-discharge testing of  $\text{LiNi}_{0.5}\text{Mn}_{1.5}\text{O}_4$  electrodes. The cells were cycled at  $20 \text{ mA g}^{-1}$  in  $1 \text{ M LiPF}_6$  in EC/DMC as an electrolyte, stored at  $25^\circ\text{C}$  for 7 d after the 10<sup>th</sup> charge, and cycled again.



**Table S1.** Eleventh-cycle coulombic efficiencies of  $\text{LiNi}_{0.5}\text{Mn}_{1.5}\text{O}_4$  electrodes with various binders obtained after self-discharge.

Binder	11 <sup>th</sup> coulombic efficiency (%)
PVdF	82.7
ALG	80.5
SO <sub>3</sub> -ALG	86.0
ester-ALG	67.0
ester-SO <sub>3</sub> -ALG	82.4

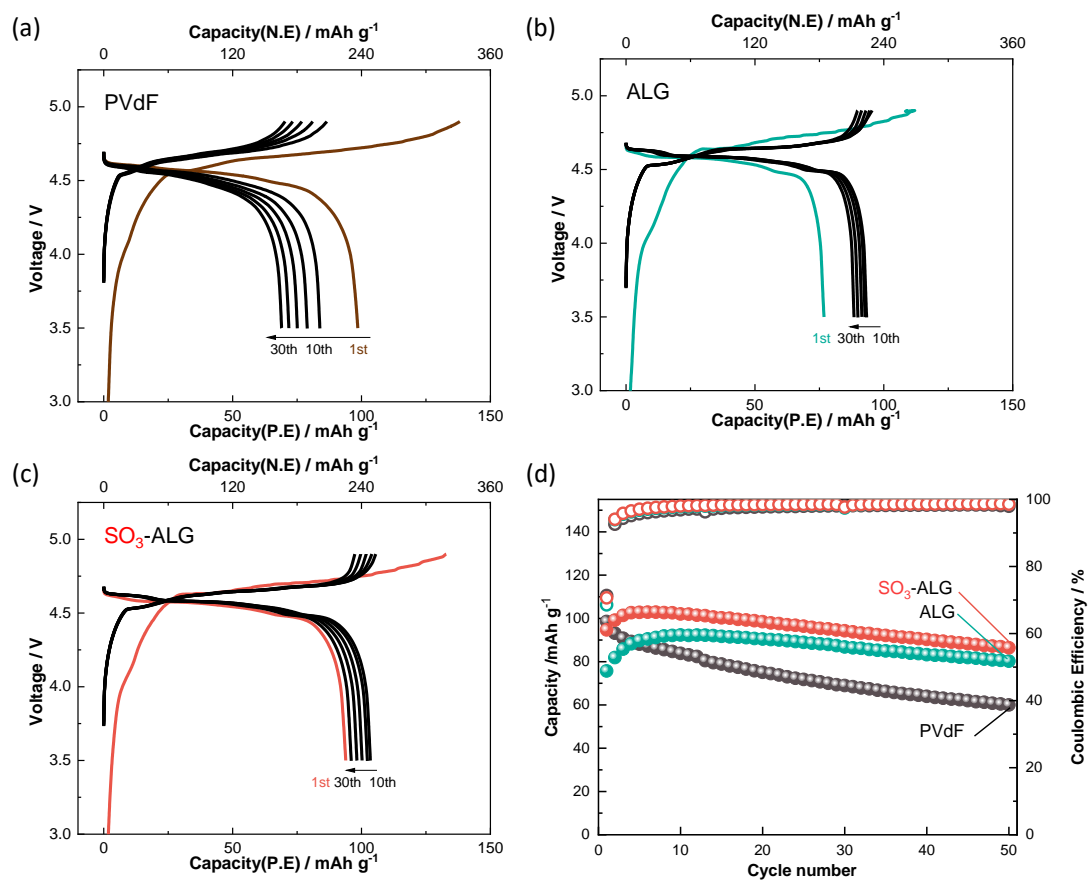


**Figure S11.** Charge–discharge curves of  $\text{LiNi}_{0.5}\text{Mn}_{1.5}\text{O}_4//\text{graphite}$  full cells with (a) PVdF, (b) ALG, and (c)  $\text{SO}_3\text{-ALG}$ . (d) Cycling performances and Coulombic efficiencies of LNMO//graphite full cells with PVdF and alginate binders. The cells were cycled at  $20 \text{ mA g}^{-1}$  in  $1 \text{ M LiPF}_6$  in EC/DMC at room temperature within the voltage range of 3.5–4.9 V.

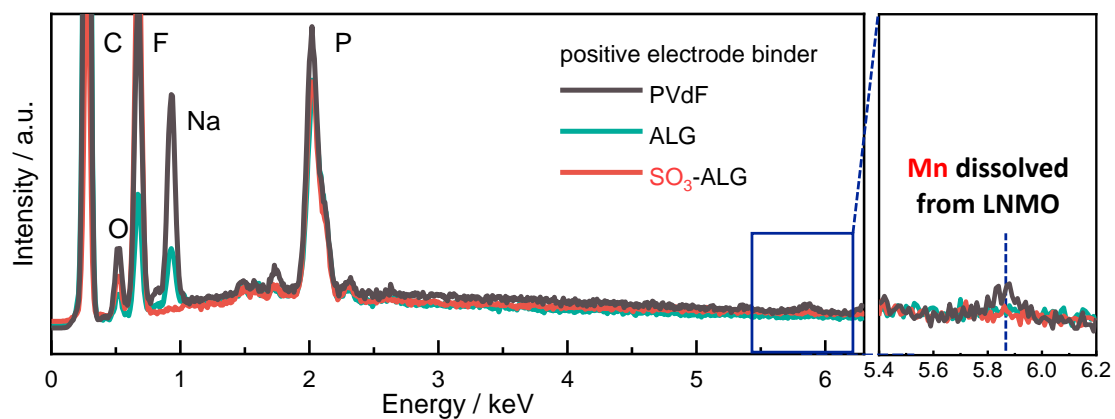


**Figure S12.** SEM-EDS profiles of graphite electrodes after 50 cycles in LNMO//graphite full cells.

**Table S2.** Surface atomic ratios estimated from the EDS profiles of graphite electrodes after 50 cycles in LNMO//graphite full cells with different binders.

Element	Positive electrode binder		
	PVdF	ALG	SO <sub>3</sub> -ALG
C	77.1	88.8	56.6
O	1.97	0.66	1.96
F	9.95	3.63	24.2
P	10.4	6.77	17.1
Mn	0.57	0.12	0.16
Total	100	100	100